Electrostatic surface trap for cold polar molecules on a chip*

Wang Qin(王 琴), Li Sheng-Qiang(李胜强), Hou Shun-Yong(侯顺永), Xia Yong(夏 勇), Wang Hai-Ling(汪海玲), and Yin Jian-Ping(印建平)†

State Key Laboratory of Precision Spectroscopy, Department of Physics, East China Normal University, Shanghai 200062, *China*

(Received 18 March 2013; revised manuscript received 5 June 2013; published 2 December 2013)

We propose a simple scheme for trapping cold polar molecules in low-field seeking states on the surface of a chip by using a grounded metal plate and two finite-length charged wires that half embanked in an insulating substrate, calculate the electric field distributions generated by our charged-wire layout in free space and the corresponding Stark potentials for ND_3 molecules, and analyze the dependence of the trapping center position on the geometric parameters. Moreover, the loading and trapping processes of cold ND_3 molecules are studied by using the Monte Carlo method. Our study shows that the loading efficiency of the trap scheme can reach 11.5%, and the corresponding temperature of the trapped cold molecules is about 26.4 mK.

Keywords: cold polar molecules, electrostatic surface trapping, Monte Carlo simulation

PACS: 37.10.Pq, 37.10.Mn, 37.10.Vz, 37.20.+j **DOI:** 10.1088/1674-1056/23/1/013701

1. Introduction

In recent years, the production and storage of cold polar molecules have attracted a great deal of interest from physicists and chemists, due to their wide and important applications, such as high-resolution spectroscopy,[1] precise measurement,[2] cold chemical reaction[3] and cold collisions,[4] quantum computing, and information processing.[5,6] So far, several methods have been developed to generate cold molecules,[7–11] and a few efficient techniques have also been developed to trap cold molecules, such as magnetic trap for cold paramagnetic molecules,[12] optical dipole trap for alkali-metal dimmers,[13] and electrostatic trap for cold polar molecules.[14] Especially for the electrostatic trap, it has been demonstrated for ND_3,[14–16] OH,[17,18] NaCs,[19] NH,[20] CO molecules,[21] etc. Our group has also made the latest contribution to this area.[22,23] Recently, Meijer's group proposed an electrostatic surface trap for metastable CO molecules and demonstrated its loading and trapping processes of cold polar molecules from a supersonic beam into a traveling potential well on a chip.[24,25] With the rapid development of the active areas like quantum computing and information processing, people demand some miniaturized surface traps that are easily being built on a substrate, so it would be worthwhile and necessary to find some new schemes to realize electrostatic surface trap for cold polar molecules on a chip.

In this paper, we propose a simple electrostatic surface trap for cold polar molecules on a chip combined with two finite-length charged wires and a grounded metal plate, and theoretically demonstrate its feasibility by Monte Carlo simulations. In Section 2, the trapping scheme for cold polar molecules in the low-field seeking (LFS) states is proposed, and several equations for calculating the electric field distribution and Stark potential for ND_3 molecules are derived. In Section 3, we calculate the diagrams of contour distribution of our charged-wire layout in the XY, XZ, and YZ planes, and analyze the dependences of the trapping center position Z_0 and the efficient trapping potential on the geometric parameters of our trap scheme. In Section 4, we study the loading and the trapping processes of cold ND_3 molecules from cold molecular beam into our surface trap by using Monte Carlo simulations, and analyze the dependences of the loading efficiency on both the loading time and the initial velocity of incident cold molecular beam. In addition, we obtain the optimal loading efficiency and its final velocity distributions of cold molecules in our surface trap. In the final section, we summarize the main results.

2. Surface trap scheme and formulas derivation

Our trapping scheme is shown in Fig. 1, which is composed of two finite-length charged wires on a Teflon substrate and a grounded metal plate. The relative dielectric constant and the insulating parameter of the Teflon material are $\varepsilon_r = 2.1$ and 60 kV/mm, respectively. Both of the two charged wires with a radius r_0 and a length l are half embanked in the upper surface of the substrate with a thickness b. The distance between the centers of the two wires is a, and the voltages U_1 and U_2 are applied to the left wire and the right wire, respectively. Due to the fringe effect of the charged wires, the ends of the two finite-length charged wires will generate two barriers, and then a three-dimensional (3D) closed potential well

*Project supported by the National Natural Science Foundation of China (Grant Nos. 10674047, 10804031, 10904037, 10974055, 11034002, and 11274114), the National Basic Research Program of China (Grant Nos. 2006CB921604 and 2011CB921602), the Basic Key Program of Shanghai Municipality of China (Grant No. 07JC14017), and the Leading Academic Discipline Project of Shanghai Municipality of China (Grant No. B408).

†Corresponding author. E-mail: jpyin@phy.ecnu.edu.cn

© 2014 Chinese Physical Society and IOP Publishing Ltd

will be formed above the surface of the substrate. Thus, the cold polar molecules in the LFS states can be trapped in this 3D potential well.

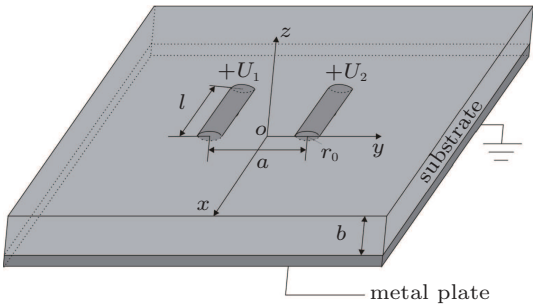


Fig. 1. Schematic diagram of electrostatic surface trapping for cold polar molecules on a chip.

According to the Poisson equation and image charge method,[26] the equations for calculating the electrostatic field distribution of our charged-wire layout can be approximately expressed as

$$E_x = -\frac{\partial \phi}{\partial x}, \tag{1}$$

$$E_y = -\frac{\partial \phi}{\partial y}, \tag{2}$$

$$E_z = -\frac{\partial \phi}{\partial z}, \tag{3}$$

where

$$\phi = \varphi_1 + \varphi_2, \tag{4}$$

and

$$\begin{aligned}\varphi_1 = & \frac{C}{4\pi\varepsilon_0(1+\varepsilon_r)} \\ & \times \left[\ln \frac{\sqrt{(l+x)^2+[(h/2)+y]^2+z^2}-(l+x)}{\sqrt{x^2+[(h/2)+y]^2+z^2}-x}\right. \\ & \left. + \ln \frac{\sqrt{(l+x)^2+[(h/2)+y]^2+(2b+z)^2}-(l+x)}{\sqrt{x^2+[(h/2)+y]^2+(2b+z)^2}-x}\right],\end{aligned} \tag{5}$$

$$\begin{aligned}\varphi_2 = & \frac{C}{4\pi\varepsilon_0(1+\varepsilon_r)} \\ & \times \left[\ln \frac{\sqrt{(l+x)^2+[(h/2)-y]^2+z^2}-(l+x)}{\sqrt{x^2+[(h/2)-y]^2+z^2}-x}\right. \\ & \left. + \ln \frac{\sqrt{(l+x)^2+[(h/2)-y]^2+(2b+z)^2}-(l+x)}{\sqrt{x^2+[(h/2)-y]^2+(2b+z)^2}-x}\right],\end{aligned} \tag{6}$$

$$h = \sqrt{a^2+4r_0^2}, \tag{7}$$

and the coefficient C is determined by the following relation:

$$\begin{aligned}&\frac{C}{4\pi\varepsilon_0(1+\varepsilon_r)}\int_{-r_0}^{-b} \\ &\times \left[-\frac{1}{z_0}-\frac{z_0}{h^2+z_0^2}+\frac{z_0}{\left(\sqrt{l^2+z_0^2}\right)\left(\sqrt{l^2+z_0^2}-l\right)}\right. \\ &\left.+\frac{z_0}{\left(\sqrt{l^2+h^2+z_0^2}\right)\left(\sqrt{l^2+h^2+z_0^2}-l\right)}\right]\mathrm{d}z_0 = U.\end{aligned} \tag{8}$$

Then, the total electric filed distribution is given by

$$|\boldsymbol{E}(x,y,z)| = \sqrt{E_x^2+E_y^2+E_z^2}. \tag{9}$$

From Eqs. (1)–(9), we can calculate the spatial distribution of the electric field, $|\boldsymbol{E}(x,y,z)|$, in free space around our charged wires layout, and analyze the relationships between the electric field $|\boldsymbol{E}(x,y,z)|$ and the geometric parameters (a,b,r_0) of the trapping system.

Due to dc Stark effect, when a polar molecule with a permanent electric dipole moment $\boldsymbol{\mu}$ moves in an inhomogeneous electrostatic filed, it will experience a dipole gradient force from the electrostatic field, which can be used to guide or trap cold polar molecules in the LFS states.

The interacting Stark potential for cold polar molecules in an inhomogeneous electrostatic field can be written as

$$W_{\text{stark}} = -\boldsymbol{\mu}\cdot\boldsymbol{E}. \tag{10}$$

For cold ND_3 molecules in the LFS states, the trapping potential can be approximated as

$$W_{\text{stark}}(r) = -\frac{M\Omega}{J(J+1)}\mu\,|E(r)|, \tag{11}$$

where J is the total angular momentum quantum number of the molecules, Ω and M are the projections of the total angular momentum J on the molecular axis and the space-fixed axis (i.e., the external field direction), respectively.

Thus, the corresponding dipole gradient force of the electrostatic field on the cold polar molecules is given by

$$\boldsymbol{F} = -\nabla W_{\text{stark}}, \tag{12}$$

and then the LFS molecules will be repelled to the minimum of the electrostatic field by the repulsive gradient force $\boldsymbol{F}$.

3. Theoretical calculation and analysis

3.1. Calculation of contour distributions of electrostatic trapping field

Figures 2(a), 2(b), and 2(c) show the corresponding E-field contours for $a = 9$ mm, $b = 5$ mm, $r_0 = 2.5$ mm, $l = 8$ mm, and $U_1 = U_2 = 15$ kV by a commercial finite element software. From Eqs. (1)–(9), the contours of the electric field generated by the charged-wire layout with the same parameters are plotted in Figs. 2(d), 2(e), and 2(f). From these figures, we can see that our analytically calculated results from

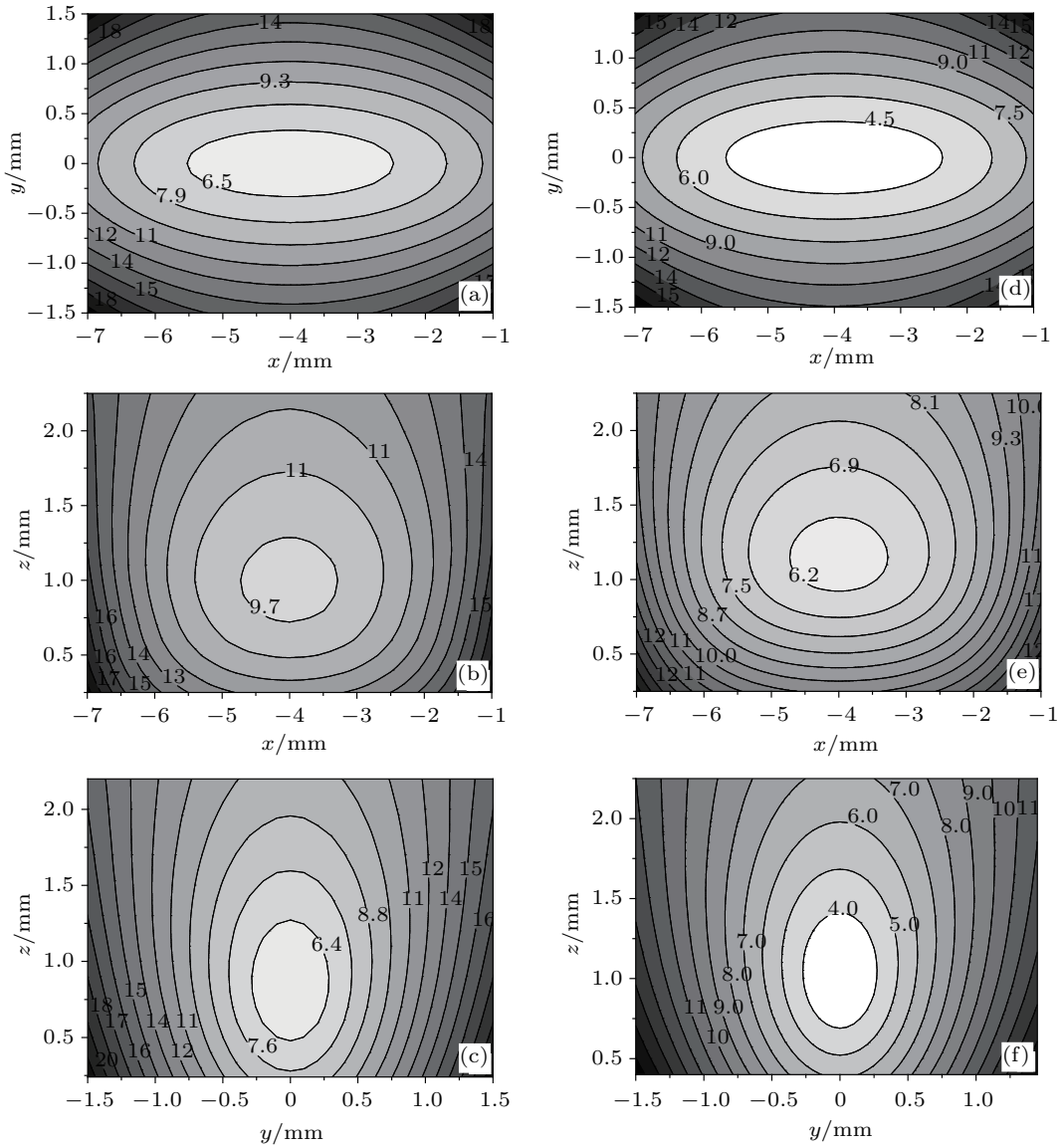


Fig. 2. The calculated contours of the electric field distribution in the XY, XZ, and YZ planes with the same parameters ($a = 9$ mm, $b = 5$ mm, $r_0 = 2.5$ mm, $l = 8$ mm, and $U_1 = U_2 = 15$ kV) by using two different methods: (a)-(c) a finite element software; (d)–(f) analytical results. The corresponding E-field values are shown in contours in units of kV/cm.

Eqs. (1)–(9) are slightly smaller than that calculated by using the commercial finite element software, but their shapes are substantially the same. Furthermore, the electrostatic field produced by the charged electrodes is a 3D closed hollow E-field distribution with a central minimum value of $|\boldsymbol{E}(x,y,z)|$, which can be used to trap cold polar molecules in the LFS states.

3.2. Dependences of trapping center position Z_0 on geometric parameters

In order to manipulate and control cold molecules in our trap, we study the dependences of the trapping-center position Z_0 (i.e., the position of the minimum electric field) on the geometric parameters (a, b, r_0) of our trap scheme, and the calculated results are shown in Fig. 3. It is clear from Fig. 3(a) that with the increase in a, the position Z_0 will be almost linearly increased. For example, when $b = 5$ mm, $r_0 = 2.5$ mm,

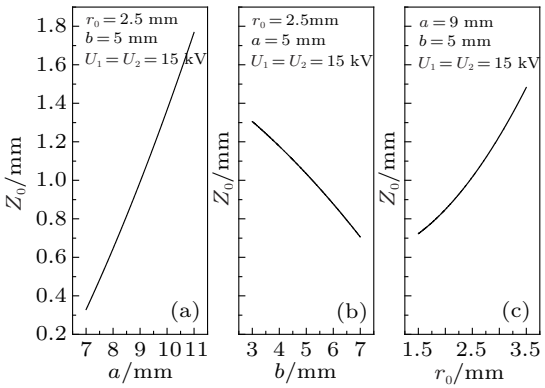


Fig. 3. Dependence of the position Z_0 of the trapping center on (a) the center-to-center space a of the two wires, (b) the thickness b of the insulating substrate, and (c) the radius r_0 of the wire.

$U_1 = U_2 = 15$ kV and a is increased from 7 mm to 11 mm, the position Z_0 will be lifted from 0.32 mm to 1.75 mm. Figure 3(b) shows that with the increase in b, the position Z_0

will be decreased rapidly. In particular, when $a = 9$ mm, $r_0 = 2.5$ mm, $U_1 = U_2 = 15$ kV, and b increases from 3 mm to 7 mm, the position Z_0 will be decreased from 1.31 mm to 0.69 mm. Figure 3(c) shows that the position Z_0 is gradually increased with the increase in the wire radius r_0. When $a = 9$ mm, $b = 5$ mm, $U_1 = U_2 = 15$ kV, and r_0 is increased from 1.5 mm to 3.5 mm, the position Z_0 will be lifted from 0.72 mm to 1.48 mm. These results show that cold polar molecules in our trap can be manipulated and controlled by changing the geometric parameters, or the trapping-center position of cold molecules on the chip surface can be designed by using the above dependences.

3.3. Dependences of efficient trapping potential on geometric parameters

Using Eqs. (1)–(11), we calculate the spatial distributions of the electrostatic fields generated by our charged-wire layout for different geometric parameter (a, b, r_0) of our trap scheme and its trapping-potential distributions for ND_3 molecules in the x, y, and z directions, and study the dependences of the efficient trapping depth on the geometric parameters (a, b, r_0). The results are shown in Fig. 4. It can be found from Fig. 4(a) that larger radius r_0 of the charged wire is accompanied by lower gradient of electric field, and also lower maximum trapping electric-field $E(x)$ (or the Stark trapping-potential depth $U(x)_{\text{stark}}$) in the x direction. We also find that the electric field $E(x)$ has two maximum values, which are located symmetrically at the edges of the two wires. The minimum value of $E(x)$ in the x direction is at the geometric center of the charged wires, and the electric field $E(x)$ will be increased rapidly with the increase in the absolute value of the x coordinate. Figure 4(b) shows that with the increase in the y coordinate, the electric field $E(y)$ (or the Stark trapping potential $U(y)_{\text{stark}}$) in the y direction will be linearly increased, which is somewhat like a quadrupole field. Figure 4(c) indicates that (i) with the increase in the radius r_0, the position Z_0 of the minimum electric field will be lifted in the z direction, but the gradient of the electric field $E(z)$ will be decreased; (ii) there are two maximum values of the electric field $E(z)$, one is at the surface of the insulting substrate, and the other is above the minimum point Z_0 of the electric field. The smaller one of these two maximal values is defined as the effective trapping electric field, and the corresponding Stark trapping potential is defined as the efficient well depth. When $a = 9$ mm, $b = 5$ mm, $r_0 = 2.5$ mm, and $U_1 = U_2 = 15$ kV, we obtain the maximum electric field $E(x)_{\max} \approx 1.4 \times 10^6$ V/m in the x direction and the corresponding trapping potential $U(x)_{\max} \approx 253$ mK at $y = 0$ and $z = z_0$; the maximum electric field $E(y)_{\max} \approx 1.5 \times 10^6$ V/m in the y direction and the corresponding trapping potential $U(y)_{\max} \approx 270$ mK at $x = -4$ and $z = z_0$; and the maximum electric field $E(z)_{\max} \approx 8 \times 10^5$ V/m in the z direction and the corresponding trapping potential $U(z)_{\max} \approx 154$ mK at $x = -4$ and $y = 0$. These results show that the electric field distributions of our proposed trap in the x, y, and z directions and their Stark trapping depths are not identical and asymmetry, and the efficient trapping depth is about 154 mK, which will be determined by the minimal efficient trapping potential in the x, y, and z directions. It is clear that such an efficient trapping depth ($\sim$154 mK) is high enough to trap cold polar molecules loaded from a Stark-decelerated molecular beam with a temperature of about 10 mK,[27] or a cw cold molecules beam with a temperature of about 50 mK from an energy low-pass filter based on a bent electrostatic guiding.[9]

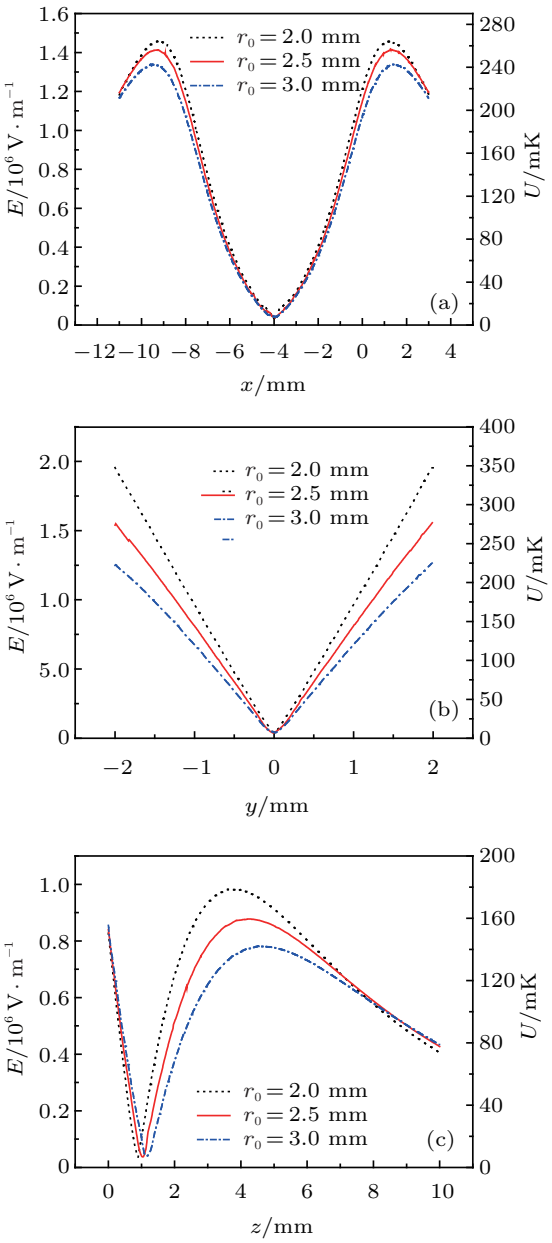


Fig. 4. (color online) The E-field distributions of our charged-wire layout and its Stark trapping potential ones for ND_3 molecules in the (a) x (at $y = 0$, $z = z_0$), (b) y (at $x = -4$, $z = z_0$), and (c) z (at $x = -4$, $y = 0$) directions for $a = 9$ mm, $b = 5$ mm, and $U_1 = U_2 = 15$ kV.

4. Loading efficiency and Monte Carlo simulations

4.1. Efficient loading of cold polar molecules

To make efficient loading of cold molecules from a cold molecular beam into our surface trap, we cut a 2-mm-diameter entrance hole so as to enable the molecular beam to enter the trap, and then our improved trap scheme is shown in Fig. 5.

For the transverse and longitudinal focusing of the beam, the electric field distribution from $y = -7$ mm to 0 mm is very important (see Figs. 5(a) and 5(c)). In this region, the molecules in the LFS states will experience a repulsive electric dipole force. Thus, when the loaded molecules move in the electric field, they have to climb a last potential hill, and will be first brought to a standstill, and then reflected back by this repulsive electric dipole force. When the slowed molecules reach the vicinity of trapping center, the voltage on the two wires will be suddenly switched (see Figs. 5(b) and 5(d)), the cold molecules will be confined in our trap. We define the time to load cold molecules exiting from the last stage of Stark decelerator into the trapping region as t_{loading}. At this moment, we quickly increase the voltage value on the left wire from 2 kV to 15 kV, that is, the same voltages ($U_1 = U_2 = 15$ kV) are applied to the two wires, and a symmetrical electrostatic field distribution with a minimum E-field value at the geometrical center of the trap is generated, and then cold molecules are efficiently loaded into the trap. We also use the Monte Carlo method to simulate the dynamical loading and trapping processes of cold ND_3 molecules, and will discuss the loading efficiency of the cold molecules and its velocity distributions in the trap in detail below.

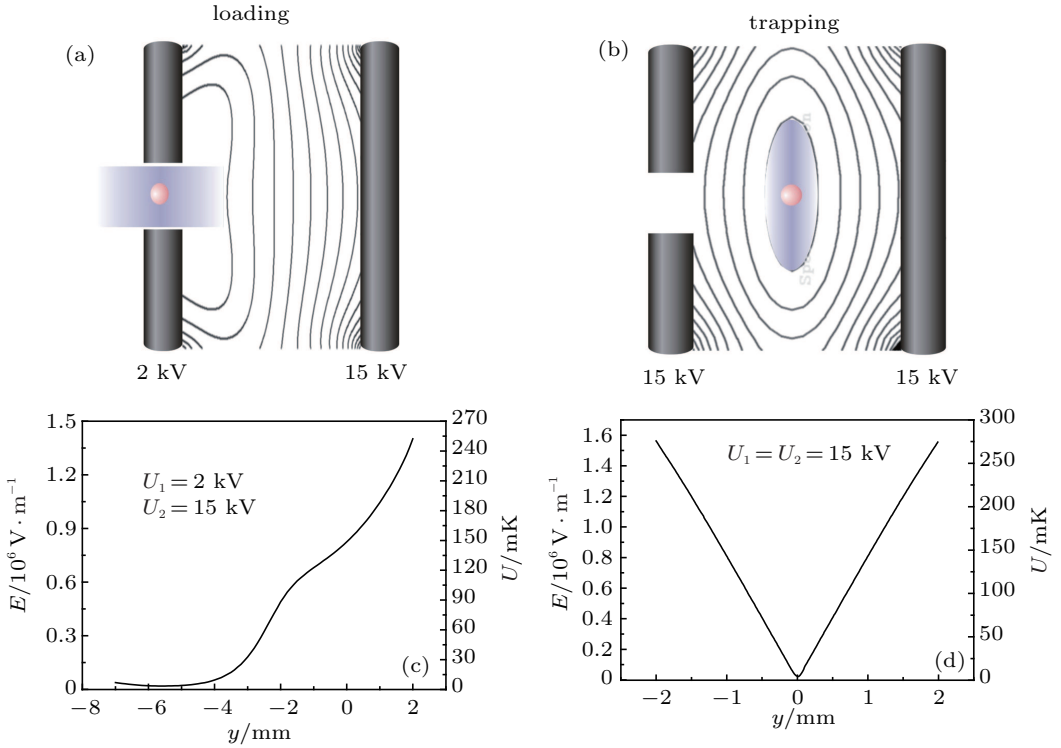


Fig. 5. (color online) (a) Schematic diagram of the two charged wires used for efficient loading of cold molecules and 2D contour distributions of the loading electric field in the XY plane. (c) The corresponding E-field and Stark loading-potential profiles for ND_3 molecules in the $|J,K\rangle = |1,-1\rangle$ state in the y direction. Similarly, (b) and (d) are used for trapping cold ND_3 molecules in the LFS states.

4.2. Loading efficiency and the velocity distributions of cold ND_3 molecules

To better understand the loading and trapping behaviors of cold molecules, we perform Monte Carlo simulations for the loading and trapping processes of cold ND_3 molecules in the state $|J,K\rangle = |1,-1\rangle$ from an incident cold molecular beam into our trap, and the simulated results are shown in Fig. 6. In our simulations, we suppose that cold ND_3 molecular beam has an initial longitudinal central velocity of 11.5 m/s (12.5 m/s or 13.5 m/s) and a spread of 3 m/s, and its transverse velocity is centered at zero with a spread of 3 m/s. The simulated molecular number is $N = 1 \times 10^5$. From Fig. 6, we can find that with the increase in the loading time, the loading efficiency of cold molecules is first increased to its maximum value, and then decreases. This means that there is the maximum loading efficiency at an optimal loading time for a given initial longitudinal velocity of the incident molecular beam. For example, when the initial longitudinal velocity is 12.5 m/s, and the optimal loading time is about 0.828 ms, the maximum loading efficiency can reach 11.5%, and the temperature of

cold molecules in our trap is about 26.4 mK. For the different initial longitudinal velocity of incident molecular beam, there is a different maximum loading efficiency and a corresponding optimal loading time. For example, when the initial longitudinal velocities of incident ND_3 beam are 11.5 m/s, 12.5 m/s, and 13.5 m/s, respectively, the maximum loading efficiencies (and optimal loading times) are 10.6% (0.843 ms), 11.5% (0.829 ms), and 9.5% (0.781 ms).

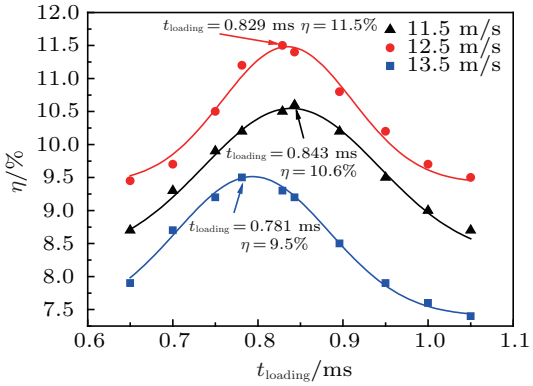


Fig. 6. (color online) Dependences of the loading efficiency of cold molecules on the loading time for different initial longitudinal velocities of incident ND_3 beam. The data points are the simulated results and the solid line is the fitted ones.

In our simulations, we do not consider any molecular loss mechanism (the collisions of cold molecules with background gas, cold collisions between the trapped molecules, etc.) due to a lower density of cold molecules in the trap.

Finally, the initial and final velocity distributions of the trapped ND_3 molecules in the x, y and z directions can be obtained from our simulations. In our simulations, the geometric parameters and the applied voltages are set as $a = 9$ mm, $b = 5$ mm, $r_0 = 2.5$ mm, $l = 8$ mm, and $U_1 = U_2 = 15$ kV, respectively. We assume that the incident molecular beam has a longitudinal velocity centered at 12.5 m/s with a velocity spread of 3 m/s, and a transverse velocity centered at zero with a spread of 3 m/s. We also choose an appropriate time step of 0.1 μs to track the trajectory of each molecule, and detect the position and velocity distributions of cold molecules at any moment. After a trapping time of 0.1 s, we analyze the velocity distributions of the trapped cold molecules in the x, y, and z directions, respectively, and compare the initial and final velocity distributions of cold molecules in the trap, and the simulated results are shown in Fig. 7. It is clear from Fig. 7(b) that the incident ND_3 beam with a longitudinal central velocity of 12.5 m/s are brought to a standstill during the loading process of cold molecules, and a cold molecular sample with a temperature of 26.4 mK can be obtained in our surface trap. These results show that our proposed trap scheme is feasible and can be used to trap cold polar molecules with a temperature of about 25 mK.

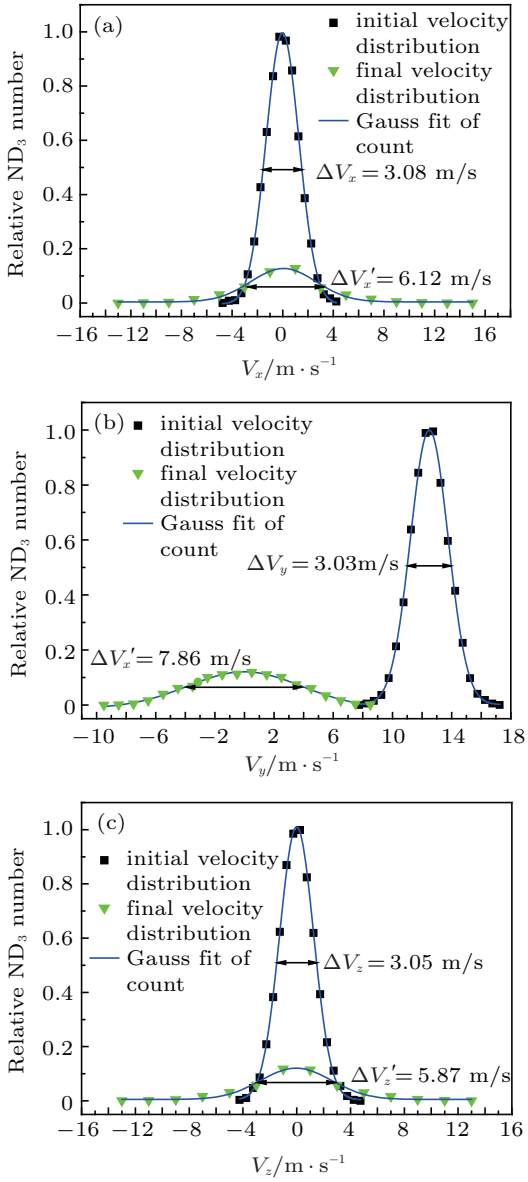


Fig. 7. (color online) The initial and final velocity distributions of the trapped cold ND_3 molecules in the (a) x, (b) y, and (c) z directions.

5. Conclusions

In this paper, we have proposed a simple electrostatic surface trapping scheme for cold polar molecules on a chip by using the two finite-length charged wires and a grounded metal plate, and calculated the corresponding electric field distribution and the Stark trapping potential for ND_3 molecules. We have also analyzed the dependences of the trapping center position Z_0 and the effective trapping potential on the geometric parameters of our charged-wire layout, studied the dynamic loading and trapping processes of cold molecules by using Monte Carlo method, and obtained the optimal trapping efficiency and the initial and final velocity distributions of cold molecules in the trap. Our studies show that when the initial longitudinal velocity of incident ND_3 molecule is 12.5 m/s and the loading time is 0.829 ms, the maximum loading efficiency can reach 11.5%, and the temperature of the trapped

cold molecules is about 26.4 mK.

In recent years, our group has proposed several schemes to guide cold polar molecules in the LFS states on the surface of a chip,[28–30] and they have been realized successfully in the experiments.[29,30] Because our trap scheme can be miniaturized and integrated easily on a chip, so our surface trap scheme has some important applications in the fields of cold molecular physics and molecule optics, integrated molecule optics and molecular chip, cold chemical reaction[3] and cold collisions,[4] even quantum computing and quantum information processing,[5,6] etc. In particular, our surface trap scheme may be used to form a novel surface Stark decelerator with an electrostatic guiding function on a chip.

References

[1] Thorpe M J, Moll K D, Jones R J, Safdi B and Ye J 2006 *Science* **311** 1595

[2] Hudson J J, Sauer B E, Tarbutt M R and Hinds E A 2002 *Phys. Rev. Lett.* **89** 023003

[3] Singh V, Hardman K S, Tariq N, Lu M J, Ellis A, Morrison M J and Weinstein J D 2012 *Phys. Rev. Lett.* **108** 203201

[4] Willitsch S, Bell M T, Gingell A D, Procter S R and Softley T P 2008 *Phys. Rev. Lett.* **100** 043203

[5] Soderberg K A B, Gemelke N and Chin C 2009 *New J. Phys.* **11** 055022

[6] Ni K K, Ospelkaus S, Wang D, Quéméner G, Neyenhuis B, deMiranda M H G, Bohn J L, Ye J and Jin D S 2010 *Nature* **464** 1324

[7] Bethlem H L, Berden G and Meijer G 1999 *Phys. Rev. Lett.* **83** 1558

[8] Weinstein J D, deCarvalho R, Guillet T, Friendrich B and Doyle J M 1998 *Nature* **395** 148

[9] Rangwala S A, Junglen T, Rieger T, Pinkse P W H and Rempe G 2003 *Phys. Rev. A* **67** 043406

[10] Wiederkehr A W, Schmutz H, Motsch M and Merkt F 2012 *Mol. Phys.* **110** 1807

[11] Fulton R, Bishop A I, Scheneider M N and Barker P F 2006 *Nat. Phys.* **2** 465

[12] Weinstein J D, de Carvalho R, Guillet T, Friedrich B and Doyle J M 1998 *Nature* **395** 148

[13] Takekoshi T, Patterson B M and Knize R J 1998 *Phys. Rev. Lett.* **81** 5105

[14] Bethlem H L, Berden G, Crompvoets F M H, Jongma R T, van Roij A J A and Meijer G 2000 *Nature* **406** 491

[15] Crompvoets F M H, Bethlem H L, Jongma R T and Meijer G 2001 *Nature* **411** 174

[16] van Veldhoven J, Bethlem H L and Meijer G 2005 *Phys. Rev. Lett.* **94** 083001

[17] van de Meerakker S Y T, Smeets P H M, Vanhaecke N, Jongma R T and Meijer G 2005 *Phys. Rev. Lett.* **94** 023004

[18] Sawyer B C, Lev B L, Hudson E R, Stuhl B K, Lara M, Bohn J L and Ye J 2007 *Phys. Rev. Lett.* **98** 253002

[19] Kleinert J, Haimberger C, Zabawa P J and Bigelow N P 2007 *Phys. Rev. Lett.* **99** 143002

[20] Hoekstra S, Metsälä M, Zieger P C, Scharfenberg L, Gilijamse J J, Meijer G and van de Meerakker S Y T 2007 *Phys. Rev. A* **76** 063408

[21] Gilijamse J J, Hoekstra S, Meek S A, Metsälä M, van de Meerakker S Y T, Meijer G and Groenenboom G C 2007 *J. Chem. Phys.* **127** 221102

[22] Xu X Y, Chen H B and Yin J P 2009 *Acta Phys. Sin.* **58** 1563 (in Chinese)

[23] Xia Y, Yin Y L, Ji X and Yin J P 2012 *Chin. Phys. Lett.* **29** 053701

[24] Meek S A, Bethlem H L, Conrad H and Meijer G 2008 *Phys. Rev. Lett.* **100** 153003

[25] Meek S A, Conrad H and Meijer G 2009 *Science* **324** 1699

[26] Hayt W H and Buck J A 2001*Engineering Electromagnetics* (6th edn.) (New York: McGraw-Hill)

[27] Bethlem H L, van Roij A J A, Jongma R R and Meijer G 2002 *Phys. Rev. Lett.* **88** 133003

[28] Deng L Z, Xia Y and Yin J P 2007 *Chin. Phys.* **16** 707

[29] Xia Y, Yin Y L, Chen H B, Deng L Z and Yin J P 2008 *Phys. Rev. Lett.* **100** 043003

[30] Deng L Z, Liang Y, Gu Z X, Hou S Y, Li S Q, Xia Y and Yin J P 2011 *Phys. Rev. Lett.* **106** 140401